Available online at www.sciencedirect.com

ScienceDirect

Energy Procedia 129 (2017) 754–761

Energy Procedia

www.elsevier.com/locate/procedia

IV International Seminar on ORC Power Systems, ORC2017
13-15 September 2017, Milano, Italy

Working Fluid Selection and Optimal Power-to-Weight Ratio for ORC in Long-Haul Trucks

Roberto Pili[a]*, Castro Pastrana Jesus D.[a], Alessandro Romagnoli[b], Hartmut Spliethoff[a], Christoph Wieland[a]

[a]*Institute for Energy Systems, School of Mechanical Engineering, Technical University of Munich, Boltzmannstr. 15, 85748 Garching, Germany*
[b]*School of Mechanical & Aerospace Engineering, College of Engineering, Nanyang Technological University (NTU), 50 Nanyang Avenue, 637820 Singapore*

Abstract

In 2013, about 82% of the total CO_2 emissions from transportation systems in the U.S. were caused by road transportation, highly based on internal combustion engines (ICE). Organic Rankine Cycles (ORC) are a waste heat recovery (WHR) technology that can contribute significantly to reduce environmental impact of road transportation. A trade-off has to be found between the improved fuel energy utilization and the weight and volume of the ORC, which increase the vehicle load and reduce the available space for transportation. In the present work, 17 working fluids are analyzed as possible candidates for WHR with direct-evaporation ORC in long-haul trucks. The preheater/evaporator is modelled as a finned shell-and-tube heat exchanger, while the condenser is an air-cooled finned flat-tube heat exchanger, as in common truck radiators. The ORC process is optimized for each fluid in terms of maximum power output, taking into account the impact of the working fluid on the heat exchanger weight and volume. The heat exchangers are modelled in MATLAB®. The results show that acetone and ethanol can recover more than 6 kW of mechanical power, but the system would present large weight and required space. Isobutane shows the highest power-to-weight and power-to-volume ratio (234 W/kg and 277 W/dm^3 resp.), but the net power output is lower. Cyclopentane and pentane allow a good trade-off between power output and space requirement. The discussed procedure can be also applied to other transportation systems, where the condenser might have to be adapted to different boundary conditions.

Peer-review under responsibility of the scientific committee of the IV International Seminar on ORC Power Systems.

Keywords: Organic Rankine Cycle; truck; heat exchanger; weight; volume; mobile

* Corresponding author. Tel.: + 49 89 289 16312; fax: + 49 89 289 16271.
E-mail address: roberto.pili@tum.de

1876-6102
Peer-review under responsibility of the scientific committee of the IV International Seminar on ORC Power Systems.
10.1016/j.egypro.2017.09.116

1. Introduction

In the United States, the transportation sector accounted for 26% of the greenhouse gas emissions in 2014 [1]. The largest source of CO_2 emissions in this sector is road transportation, highly based on diesel and gasoline internal combustion engines (ICE), which accounted for about 82% of the total transportation emissions in 2013 [2]. Since 80% of the goods in the U.S. are hauled by means of long-haul trucks, measures to reduce the fuel consumption and emissions of long-haul trucks are of major importance [3]. The two goals might counteract each other; studies report that the increase in efficiency of heavy-duty vehicles has been slowed down by e.g. $DeNO_x$ after-treatment [4].

A significant reduction in fuel consumption can be achieved by utilizing the waste heat, which is generally transferred to the environment by means of the exhaust gases and engine cooling system [5–7]. The exhaust gases are typically more attractive because of the higher exergy content [8]. Organic Rankine Cycle (ORC) are a valuable option to convert the waste heat into either mechanical or electrical energy [3, 9]. Recently, most of the research has been driven towards the thermodynamic and turbomachinery optimization of ORC [10–12]. The impact of the working fluid on the weight and size of the system has been instead hardly studied [13]. It has been pointed out in previous work by the authors, that weight and space requirement of the ORC system can be critical for the economic performance of the ORC integration, especially for road transportation [14]. The weight of the ORC has in fact not only a negative effect on the waste heat recovery because of the increased vehicle load, but it also represents an important indicator of the purchase costs. It is therefore interesting to compare different working fluids not only in the achievable power output, but also in the ORC compactness and weight. The present works compares the performance of different organic working fluids for waste heat recovery from ORC. The power-to-weight (PTW) and power-to-volume ratio (PTV) of different working fluids is determined for common exhaust gas conditions for heavy-duty trucks on highway. Varying driving conditions might change the net power output, and hence the effective PTW and PTV. The methodology can be also used for other applications, where weight and space availability are of major concern. In future work, the part-load behavior of the working fluids will be considered, and the results of the present analysis will be extended.

Nomenclature

ORC	Organic Rankine Cycle	C	constant	α	heat transfer coefficient
ICE	Internal Combustion Engine	H	tube/fin height	λ	thermal conductivity
PTW	Power-to-Weight	W	width	fin	finned
PTV	Power-to-Volume	T	tube d tube outer diameter	cc	counter-flow
LMTD	Logarithmic Mean Temp. Diff.	t	wall thickness	cf	cross-flow
Re	Reynolds number	p	operating pressure	k	condensation
Pr	Prandtl number	σ	material ultimate tensile strength	fg	flue gas
A	surface area	η_{fin}	fin efficiency	g0	tube bare surface

2. Waste Heat Recovery from Long-Haul Trucks with ORC

More than 99% of the heavy-duty trucks in Germany are driven by diesel engines [15]. The main waste heat sources of diesel engines consist of the engine jacket coolant and the exhaust gas, which can be found either on the exhaust pipe or in the Exhaust Gas Recirculation loop (EGR) [7, 8]. All the heat sources can be coupled and recovered in an ORC power system. The coupling is however challenging for system control, to ensure optimal cooling of the main engine, and to keep as low as possible weight and space requirements. A summary of the proposed waste heat recovery configurations with ORC can be found in [16]. To reduce system complexity and achieve light and compact design, only the flue gas will be considered as heat source for the ORC in the present analysis. The layout of a simple ORC is shown in Fig. 1. The main components are the preheater/evaporator, where the working fluid is vaporized by cooling down the flue gas; an expander, where the thermal energy of the fluid is converted into mechanical power; a condenser, which condenses the working fluid and a pump, which forwards the working fluid to the evaporator to close the thermodynamic cycle. The ORC might also be equipped with a recuperator, which heats up the liquid at the pump outlet by cooling down the vapor leaving the expander, before it is condensed. This can result in a higher efficiency,

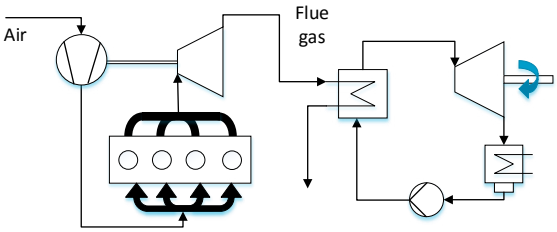

Fig. 1. Waste heat recovery of a turbocharged engine with simple ORC.

especially for dry fluids [17] . It is worth mentioning that the recuperator is a gas/liquid heat exchanger, and it might require large heat transfer surfaces. Since its integration increases the weight and volume of the ORC, only a non-recuperated ORC as in Fig. 1 is considered in the following. In future works, also recuperated ORCs will be considered.

3. Model development and simulation

This section describes the methodology used in the present work. The ORC is firstly thermodynamically optimized for maximum net power, and the thermodynamic results are subsequently used to design the heat exchangers, which are optimized for minimum weight. The flue gas properties are taken from [18].

The ORC is thermodynamically optimized by means of an in-house code written in MATLAB® and validated with Ebsilon®Professional. Once the temperature, mass flow rate and chemical composition of the heat source are known, the optimal turbine inlet pressure and temperature are defined for a given working fluid. The objective function is the ORC net power output P_{net}, which must be maximized:

$$P_{net} = P_e - P_p = \dot{m}(h_{e,in} - h_{e,out,s})\eta_e + \frac{\dot{m}(h_{p,in} - h_{p,out,s})}{\eta_p} \quad (1)$$

where P is the power output, ṁ is the mass flow rate, h is the specific enthalpy, η is the efficiency and the subscripts ‘e’, ‘p’, ‘s’, ‘in’ and ‘out’ refer respectively to the expander, pump, isentropic transformation, inlet and outlet. Due to relatively novel interest in expanders for mini-ORCs and the peculiar unconventional behavior of organic fluids, accurate correlations describing the efficiency of ORC expanders are not well established. Therefore, the code assumes constant expander and pump efficiency and a given minimum pinch-point temperature difference for each fluid (see Table 1). Since the condensing temperature can have a large impact on the condenser heat exchanger surface, the analysis is carried out for three different condensing temperatures (30-50°C [7, 13]). Notice that some works propose condensing temperatures above 60°C because of the utilization of an intermediate cooling loop [9] and/or because of more extreme environmental conditions (low vehicle speed and higher ambient temperatures [19]). In this work, the focus is on driving conditions on highway and relatively mild ambient temperature (20°C). In extreme cases, a fan might be required to ensure full condensation. No electrical generator is considered, since the ORC expander might directly transfer all the mechanical power to the main engine shaft. Pressure drops in heat exchangers and pipes are neglected in the optimization tool. The maximum inlet turbine pressure is equal to 80% of the critical pressure and lower or equal to 30 bar [20], and the minimum condensing pressure p_k is set at 1 bar, as summarized in Table 1.

The evaporator considered in this analysis is a finned shell-and-tube heat exchanger, where the flue gas flows on the shell side, and the working fluid is vaporized inside steel tubes (see Fig. 2a). The considered arrangement is cross counter-flow, as described in [21]. The tubes are considered as circular, and an in-line arrangement is preferred to the staggered to limit the pressure drop on the flue gas side. The fins are assumed to be circular. Pipe thickness t has a significant impact on the weight of the heat exchanger, and therefore adjusted as a function of the evaporation pressure,

Table 1. Model assumptions for thermodynamic optimization.

Quantity	Unit	Value	Quantity	Unit	Value
Min. heat source temperature	[°C]	150	Turbine efficiency	[%]	75
Pinch-point temperature difference	[K]	10	Condensation temperature range	[°C]	max(30-50°C, sat. temp. at 1 bar)
Pump efficiency	[%]	70	Maximum evaporation pressure	[bar]	min(80% critical pressure, 30 bar)

according to the equation [22]:

$$t = \frac{p_{ev} d}{2\sigma + p_{ev}} + 0.005d + 0.001 \tag{2}$$

where p is the fluid pressure, d the external pipe diameter, and σ the material ultimate tensile strength (set to 807 MPa for 304L steel). According the pipe outer diameter, a minimum thickness is set as a function of the tube diameter [23]:

$$\begin{aligned} t_{\min} &= 0.0012m && d < 0.016m \\ t_{\min} &= 0.0017m && \text{for} \quad 0.016m < d < 0.019m \\ t_{\min} &= 0.0021m && d > 0.019m \end{aligned} \tag{3}$$

A number of 6 pipes in series are considered for the same row, as in [21]. The tube length is set to 0.3 m. Most of the heat transfer correlations are defined in the VDI Heat Atlas [24]. For the heat transfer on the flue gas side, the following correlation is used (Section G7 in [24]):

$$\alpha_{fg} = \frac{\lambda}{d} C \, \mathrm{Re}^{0.6} \, A_{g0}{}^{-0.15} \, \mathrm{Pr}^{1/3} \tag{4}$$

where λ is the thermal conductivity, Re is the Reynolds number, A_{g0} is the bare surface area of the tube with no fins, Pr is the Prandtl number and the factor C = 0.22 for in-line arrangement. The heat transfer coefficient is corrected to account for the effect of the fins:

$$\alpha_{fg,fin} = \alpha_{fg} (1 - (1 - \eta_{fin}) \frac{A_{fin}}{A}) \tag{5}$$

where η_{fin} is the fin efficiency according to Schmidt [25], A_{fin} is the fin heat transfer area and A is the total shell heat transfer area. For single-phase working fluid, Gnielinski's equation is used (Section G1 in [24]). In the transition region (2300 < Re < 10 000) the correlations for constant wall temperature are applied. For two-phase evaporation, the equation for convective flow boiling in horizontal tubes is used and integrated over a vapor quality from 0 to 1 (Section H3.4 in [24]). A correction factor for the logarithmic mean temperature difference (LMTD) is also included, to account for the multi-pass arrangement. Given the desired inlet and outlet temperature of the heat exchanger, the $LMTD_{cf}$ for cross-flow heat exchanger with mixing on one-side (the tube side) can be determined [26]. Given the number of rows n and the $LMTD_{cc}$ for a pure counter-flow heat exchanger, the LMTD for a counter cross-flow heat exchanger is expressed by [26]:

$$LMTD = LMTD_{cf}{}^{1/n} \, LMTD_{cc}{}^{(1-1/n)} \tag{6}$$

The pressure drop on the flue gas side is determined by the equation for tube bundles in cross-flow proposed by the VDI Heat Atlas (Section L1.4 in [24]). The pressure drop for the enlargement and reduction in the exhaust pipe caused by the ORC evaporator is also considered (Section L1.4 in [24]). It is assumed that the exhaust pipe of the truck has a diameter of 0.11 m. For simplicity, the pressure drop at the entrance is approximated as the one for an inlet/outlet diameter ratio equal to 1.5. For the working fluid, the pressure drop in single phase is computed by means of Colebrook's equation [27]. The tube roughness is set at 0.045 mm [23]. For the two-phase region, Friedel's equation is used [28]. The pressure drop on the working fluid side is increased by the bends and changes of direction of the fluid flow. 180° bends are considered, multiplying by 1.8 times the pressure drop for 90° bends, as suggested in [29]. The pressure drop for the flue gas is limited to 15 mbar, whereas for the working fluid the limit is set at 200 mbar. The evaporator weight includes not only the weight of the heat exchanger metal, but also the weight of the working fluid at the design point. The weight of the flue gas is neglected, since it should not influence significantly the ORC weight. The heat exchanger volume considers the outer region occupied by the heat exchanger. The optimization variable for the evaporator design are the tube outer diameter d, the fin outer diameter D, the fin thickness s and the fin pitch (s+a) (see Fig. 2a). The optimization variables are chosen so that the evaporator weight is minimized.

The condenser applied in this work is shown in Fig. 2b. As typical truck coolers, it is made of finned flat-tubes, where the working medium condenses inside the tubes, and air flows in cross-flow through the fin spacing. The plates

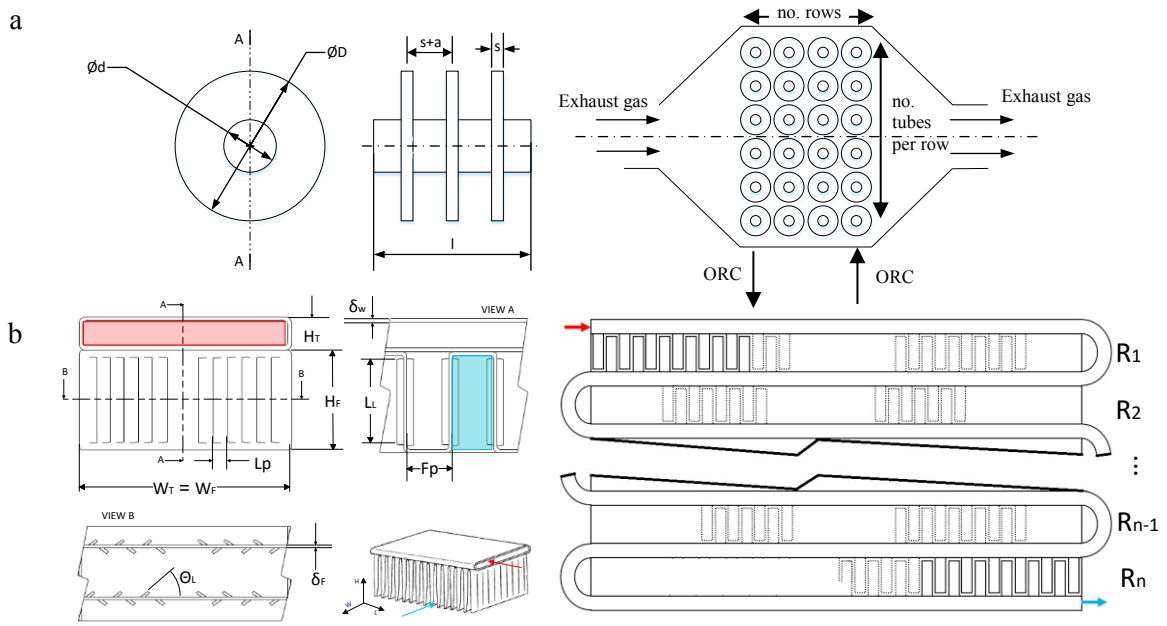

Fig. 2. (a) Finned-and-tube evaporator. (b) Finned flat-tube air-cooled condenser.

are considered aluminum rectangular plates with single channel and the fins are louvered, to improve the heat transfer. The working fluid must be completely condensed at the condenser outlet, and no subcooling is considered. The heat exchanger is discretized in cells along the working fluid path, so that the influence of the gradual change in vapor quality for the working fluid can be properly represented. The LMTD is corrected to account for a pure cross-flow arrangement, as described in Section C1 in [24]. The correlations used for the heat transfer coefficients are given in Table 2. The heat exchanger model is written in MATLAB® and optimized for minimum weight. The optimization variables are the tube width W_T, fin height H_F and fin pitch F_p. The velocity of the incoming air is fixed at 40 km/h, and the air outlet temperature and mass flow rate are found iterating on the tube length. The main geometrical assumptions are summarized in Table 3. The tube thickness is also corrected as a function of the condensation pressure p_k, by a simplified version of Eq. 1 [23]:

$$t = \frac{p_k d_h}{2\sigma} \tag{7}$$

where d_h is the tube hydraulic diameter and the minimum thickness is $t_{min} = 0.5$ mm. The pressure drop on the air side is computed making use of Kim and Bullard's correlation, and limited to 50 mbar, to reduce vehicle drag. For the working fluid, Colebrook's equation is used for single phase, whereas in the two-phase region Friedel's equation is applied, as for the evaporator. The pressure drop is also corrected to account for flow bending as in section L2.2 in [24]. The maximum pressure drop on the working fluid side is set to 100 mbar. The model (without optimization routine) is validated with the Condenser example for flat tubes in the Heat Exchanger library from Modelon [30], with error below 2% for temperatures and heat transfer rate.

4. Results

This section shows the main results from the ORC and heat exchanger design optimization. Only the core weight and volume of the heat exchangers are considered for the entire ORC, because these have the highest contribution [9]. The flue gas entering the ORC evaporator has a mass flow rate of 0.19 kg/s and a temperature of 600 K, close to the values given by [19]. Cooling air is assumed to be at 293.15 K and the input air velocity is set at 40 km/h. As shown in Fig. 3, the highest net power output is reached by acetone, followed by cyclopentane and ethanol. Acetone and ethanol show however very large weight and volume of the heat exchangers, leading to a relatively low PTW and

Table 2. Heat transfer correlations and friction factors for the condenser.

Quantity	Fluid	Unit	Correlation	Ref.
Heat transfer coefficient	Air	[W/m^{2}K]	Kim and Bullard	[31]
Heat transfer coefficient	Working fluid	[W/m^{2}K]	Single phase: Gnielinski	Sec. G1 in [24]
			Two-phase: Shah	[32]
Friction factor	Air	[-]	Kim and Bullard	[31]
Friction factor	Working fluid	[-]	Single phase: Colebrook	[27]
			Two-phase: Friedel	[28]
Friction factor over bends	Working fluid	[-]	180° bends	Sec. L2.2 in [24]

PTV ratio (<77 W/kg and 71 W/dm^3). This might not be feasible if weight and volume are strictly limited. The highest PTW and PTV ratios are reached by isobutane at 50°C condensation (234 W/kg and 277 W/dm^3), even though the power output is at this point almost half of the one with acetone. A very good compromise between power output and PTW/PTV is shown by cyclopentane, whose power output exceeds 6 kW, and PTW is higher than 160 W/kg. Also pentane performs well, with 5.4 kW at 30°C condensation and a PTW of 180 W/kg. For R218, no results could be achieved for condensing temperature at 40°C and 50°C, since the saturation pressure becomes too high. For water, toluene, MM, ethanol, hexane and acetone, the results are shown for a condensing temperature corresponding to the saturation temperature at 1 bar.

5. Conclusions

In this work, working fluid selection for waste heat recovery with ORC from long-haul trucks is analyzed, with particular attention to the influence of the working fluid on the weight and space requirement of the ORC. It has been shown that some fluids, e.g. acetone, ethanol and toluene, promise a large net power output at the design point, but require a very large size of the system. Cyclopentane and pentane can allow a good trade-off between nominal power output, weight and required space. Isobutane could reach the highest power-to-weight ratio and power-to-volume ratio, but the net power output is lower. A full applicability of the analyzed working fluid can only occur after a thorough consideration of safety and environmental issues. The procedure shown in this paper can be also applied to other transportation systems, where the condenser might have to be adapted to account for alternative cooling media and/or different boundary conditions. As part of future work, a detailed expander model will be included, the off-design behavior of the fluids will be analyzed, and an economic assessment of the waste heat recovery with ORC will be carried out.

Acknowledgements

This work is financed by the Munich School of Engineering (MSE) of the Technical University of Munich (TUM), in cooperation with the Nanyang Technological University (NTU) of Singapore.

Table 3. Geometric assumptions for the condenser.

Quantity	Symbol	Unit	Description / Value	Quantity	Symbol	Unit	Description / Value
Tube width	W_T	[m]	Optimization variable	Fin thickness	δ_F	[m]	0.00015
Tube height	H_T	[m]	1/10th of tube width	Louver length	L_L	[m]	= 0.8 H_F
Tube wall thickness	δ_W	[m]	max(Eq. 6,0.0005) (1)	Louver pitch	L_p	[m]	0.0015
Tube pitch	T_p	[m]	= H_F + δ_F	Louver angle	Θ_L	[°]	25
Fin width	W_F	[m]	= W_T	Core width	W_c	[m]	Result, max 0.9(2)
Fin height	H_F	[m]	Optimization variable	Core height	H_c	[m]	Result

(1): Wall thickness as function of tube internal pressure or 0.5 mm if lower. (2): based on Mercedes-Benz “Actros” truck radiator [33].

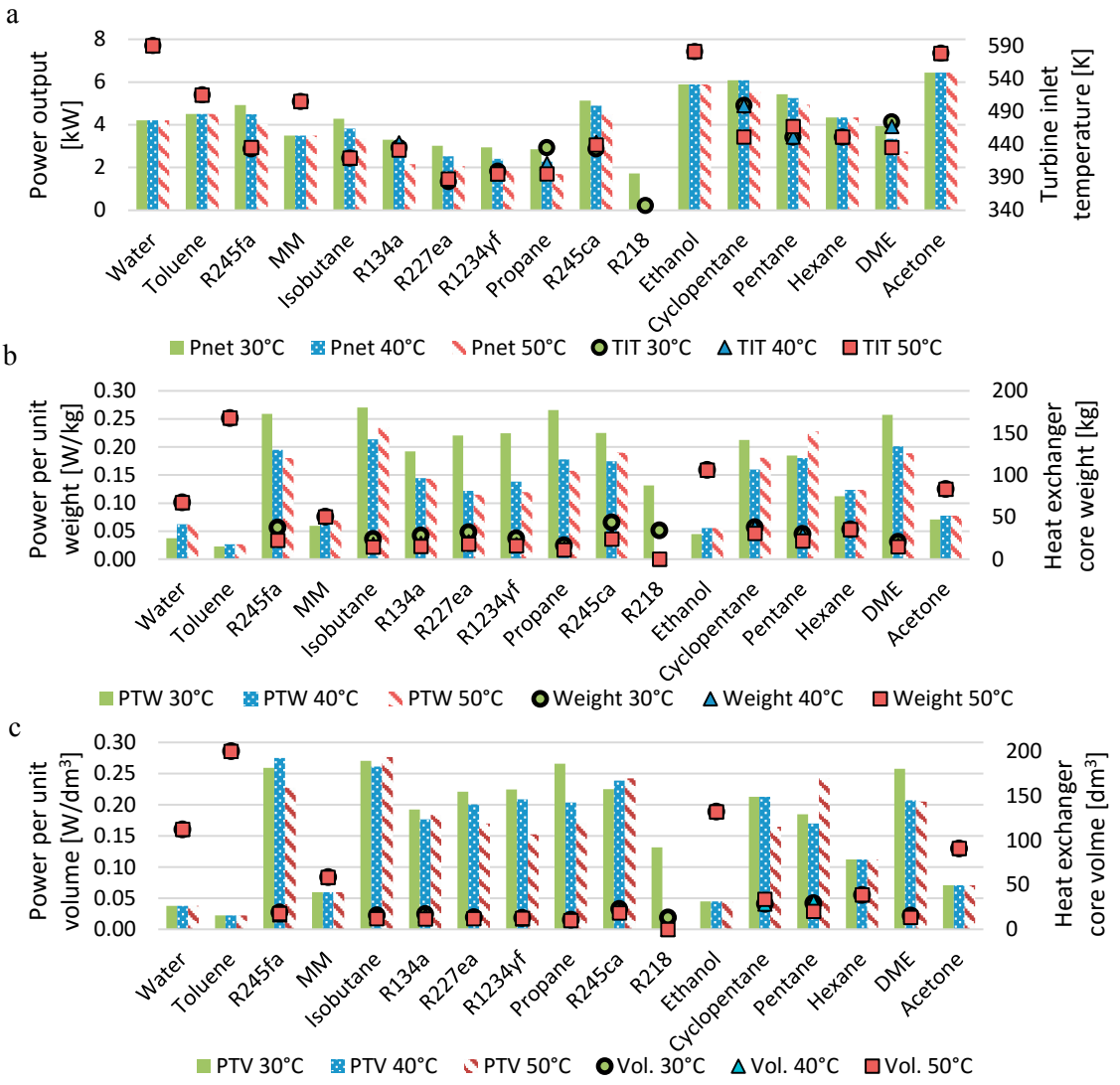

Fig. 3. Results: (a) Net power output (left axis) and turbine inlet temperature (right axis); (b) Power-to-weight (left axis) and core heat exchanger weight (right axis); (c) Power-to-volume (left axis) and core heat exchanger volume (right axis). Condensing temperature for water, toluene, MM, ethanol, hexane and acetone corresponds to the saturation temperature at 1 bar.

References

[1] EPA - U.S. Environmental Protection Agency. Inventory of U.S. Greenhouse Gas Emissions and Sinks: 1990-2015; 2017.

[2] U.S. Department of Transportation - Bureau of Transportation Statistics. Transportation Statistics Annual Report 2015. Washington DC; 2016

[3] Delgado O, Lutsey N. The U.S. Supertruck Program. Expediting the Development of Advanced Heavy-Duty Vehicle Efficiency Technologies. International Council on Clean Transportation, Washington DC; 2014.

[4] Pischinger S, Körfer T, Wiartalla A, Schnitzler J *et al.* Combined Particulate Matter and NOx Aftertreatment Systems for Stringent Emission Standards. SAE Technical Paper 2007-01-1128, 2007.

[5] Sprouse C, Depcik C. Review of Organic Rankine Cycles for Internal Combustion Engine Exhaust Waste Heat Recovery. Applied Thermal Engineering 2013; 51. p. 711–722.

[6] Odhams AMC, Roebuck RL, Lee YJ, Hunt SW, Cebon D. Factors Influencing the Energy Consumption of Road Freight Transport. Proceedings of the Institution of Mechanical Engineers, Part C: Journal of Mechanical Engineering Science 2010; 224. p. 1995–2010.

[7] Dolz V, Novella R, García A, Sánchez J. HD Diesel Engine equipped with a Bottoming Rankine Cycle as a Waste Heat Recovery System. Part 1: Study and Analysis of the Waste Heat Energy. Applied Thermal Engineering 2012; 36. p. 269–278.
[8] Bernath MG. Ganzheitliche Modellerstellung zur Wirkungsgraderhöhung von Nutzfahrzeugen durch thermische Rekuperation. Dissertation. LVK Lehrstuhl f. Verbrennungskraftmaschinen; 2016.
[9] Lang W, Colonna P, Almbauer R. Assessment of Waste Heat Recovery From a Heavy-Duty Truck Engine by Means of an ORC Turbogenerator. J. Eng. Gas Turbines Power 2013; 135(4), 042313.
[10] Guillaume L, Legros A, Quoilin S, Declaye S, Lemort V. Sizing Models and Performance Analysis of Volumetric Expansion Machines for Waste Heat recovery through organic Rankine cycles on passenger cars. 8th International Conference on Compressors and their Systems, City University London, 2013, p. 431–443.
[11] Seher, D, Lengenfelder, T, Gerhardt, J. Waste Heat Recovery for Commercial Vehicles with a Rankine Process. 21st Aachen Colloquium Automobile and Engine Technology, 2012.
[12] White M, Sayma AI. The One-Dimensional Meanline Design of Radial Turbines for Small Scale Low Temperature Organic Rankine Cycles. In: AMSE Turbo Expo 2015: Turbine Technical Conference and Exposition (V02CT42A014). ASME. ISBN: 9780791856659.
[13] Macián V, Serrano JR, Dolz V, Sánchez J. Methodology to Design a Bottoming Rankine Cycle, as a Waste Energy Recovering system in Vehicles. Study in a HDD Engine. Applied Energy 2013; 104. p. 758–771.
[14] Pili R, Romagnoli A, Spliethoff H, Wieland C. Economic Feasibility of Organic Rankine Cycles (ORC) in Different Transportation Sectors. Energy Procedia 2017; 105, p. 1401-1407.
[15] Shell Deutschland Oil GmbH, DLR. Diesel oder Alternative Antriebe - Womit fahren Lkw und Bus morgen? Fakten, Trends und Perspektiven bis 2040. Shell Nutzfahrzeug-Studie. Hamburg, 2016.
[16] Tona P, Peralez J. Control of Organic Rankine Cycle Systems on board Heavy-Duty Vehicles: A Survey. IFAC-PapersOnLine 2015; 4815. p. 419–426.
[17] Wang E, Zhang H, Fan B, Wu Y. Optimized Performances Comparison of Organic Rankine Cycles for Low Grade Waste Heat Recovery. J Mech Sci Technol 2012; 26(8). p. 2301–2312.
[18] Hatami M, Ganji DD, Gorji-Bandpy M. Numerical Study of Finned Type Heat Exchangers for ICEs Exhaust Waste Heat Recovery. Case Studies in Thermal Engineering 2014; 4. p. 53–64.
[19] Espinosa N, Tilman L, Lemort V, Quoilin S, *et al*. Rankine Cycle for Waste Heat Recovery on Commercial Trucks: Approach, Constraints and Modelling. Diesel International Conference and Exhibition. France, 2010.
[20] Quoilin S, van Broek MD, Declaye S, Dewallef P, Lemort V. Techno-Economic Survey of Organic Rankine Cycle (ORC) Systems. Renewable and Sustainable Energy Reviews, 2013; 22. p. 168–186.
[21] Zhang HG, Wang EH, Fan BY. Heat Transfer Analysis of a Finned-Tube Evaporator for Engine Exhaust Heat Recovery. Energy Conversion and Management 2013; 65. p. 438–447.
[22] American Society of Mechanical Engineers (ASME). 2010 ASME Boiler & Pressure Vessel Code, 2010.
[23] Towler GP, Sinnott RK. Chemical engineering design. Principles, Practice and Economics of Plant and Process Design, 2nd ed. Amsterdam, London: Butterworth-Heinemann, 2013.
[24] Verein Deutscher Ingenieure. VDI Heat Atlas, 2nd ed. Berlin: Springer-Verlag Berlin Heidelberg, 2010.
[25] Schmidt TE. La Production Calorifique des Surfaces Munies d'Ailettes. Bulletin De L'Institut International Du Froid Annexe G-5, 1945-46.
[26] Wagner W. Wärmeübertragung. Grundlagen.6th ed. Würzburg: Vogel, 2004.
[27] Colebrook CF. Turbulent Flow in Pipes, with particular Reference to the Transition Region between the Smooth and Rough Pipe Laws. Journal of the Institution of Civil Engineers, 1939; 114. p. 133–156.
[28] Friedel L. Druckabfall bei der Strömung von Gas/Dampf-Flüssigkeitsgemischen in Rohren. Chem.-Ing.-Tech., 1978; 503. p. 167–180.
[29] Münzinger F. Dampfkraft. Berechnung und Verhalten von Wasserrohrkesseln Erzeugung von Kraft und Wärme. Ein Handbuch für den Praktischen Gebrauch. Berlin, Heidelberg: Springer Berlin Heidelberg, 1949.
[30] Modelon AB. Heat Exchanger Library: Modelon, Lund, Sweden, 2014.
[31] Kim M, Bullard CW. Air-side Thermal Hydraulic Performance of Multi-Louvered Fin Aluminium Heat Exchangers. International Journal of Refrigeration, 2002; 25. p. 390–400.
[32] Shah MM. A General Correlation for Heat Transfer during Film Condensation inside Pipes. International Journal of Heat and Mass Transfer 2013; 224. p. 547–556.
[33] Diesel Technic AG. Spare parts catalogue for Mercedes-Benz Actros, Antos, Arocs, Atron, Axor; Version 3.0 P, p.776.